Inorg. Chem. **2006**, *45*, 7671–7680

Toward Rational Construction of Gold, Gold–Silver, and Gold–Mercury String Complexes: Syntheses, Structures, and Properties of $[Au(Tab)_2]_2L_2$ (L = I and PF_6), $\{[(Tab)_2M][Au(CN)_2]\}_2$ (M = Au and Ag), and $\{[Hg(Tab)_2][Au(CN)_2]_2\}$ [Tab = 4-(Trimethylammonio)benzenethiolate]

Jin-Xiang Chen,[†] Wen-Hua Zhang,[†] Xiao-Yan Tang,[†] Zhi-Gang Ren,[†] Hong-Xi Li,[†] Yong Zhang,[†] and Jian-Ping Lang*[,†,‡]

School of Chemistry and Chemical Engineering, Suzhou University, Suzhou 215123, Jiangsu, People's Republic of China, and State Key Laboratory of Coordination Chemistry, Nanjing University, Nanjing 210093, Jiangsu, People's Republic of China

Received April 17, 2006

The reaction of AuI with 2 equiv of TabHPF$_6$ [TabH = 4-(trimethylammonio)benzenethiol] in the presence of excess Et_3N in dimethylformamide (DMF)/MeOH afforded a binuclear gold(I) complex $[Au(Tab)_2]_2I_2\cdot 2H_2O$ (**1**). Anion exchange of **1** with NH_4PF_6 in DMF gave rise to the more soluble complex $[Au(Tab)_2]_2(PF_6)_2$ (**2**). Treatment of **2** with $K[Au(CN)_2]$ produced a tetranuclear gold(I) complex $\{[(Tab)_2Au][Au(CN)_2]\}_2$ (**3**). Analogous reactions of two known mononuclear complexes $[Ag(Tab)_2](PF_6)$ (**4**) and $[Hg(Tab)_2](PF_6)_2$ (**5**) with 1 or 2 equiv of $K[Au(CN)_2]$ generated one Ag_2Au_2 complex $\{[(Tab)_2Ag][Au(CN)_2]\}_2$ (**6**) and one Au/Hg complex $\{[Hg(Tab)_2][Au(CN)_2]_2\}$ (**7**), respectively. Compounds **1**–**3**, **6,** and **7** were fully characterized by elemental analysis, IR spectra, UV–vis spectra, ^{1}H NMR, and single-crystal X-ray crystallography. **1** and **2** have a similar $[Au(Tab)_2]_2^{2+}$ dimeric structure in which the two $[Au(Tab)_2]^+$ cations are connected via one Au–Au aurophilic interaction. In the structure of **3** or **6**, each of the two pairs of $[M(Tab)_2]^+$ cation and $[Au(CN)_2]^-$ anion is held together via ionic interactions to form a $\{[(Tab)_2M][Au(CN)_2]\}$ species (M = Au, **3**; Ag, **6**). Two such species are further connected by one Au–Au aurophilic bonding interaction to form an uncommon Au_4 or Ag_2Au_2 linear string structure with three ligand-unsupported metal–metal bonds. For **7**, the $[Hg(Tab)_2]^{2+}$ dication and the $[Au(CN)_2]_2^{2-}$ dianion are interconnected by the secondary Hg···N(CN) interactions to form a 1D chain structure. The thermal and luminescent properties of **1**–**3**, **6**, and **7** in solid state were also investigated.

Introduction

In the past decades, the rational design and construction of gold(I) complexes have received much attention because of their interesting structural chemistry and their potential applications in electronic, optical, and sensing devices.[1−5] In many gold(I) complexes, the so-called aurophilic interactions are observed to result in the formation of various interesting structures.[3] Among them, gold(I) string complexes are not exceptional, but only several examples are observed to have a linear or pseudolinear Au−Au−Au−Au structure.[1g−j] For mixed gold−silver complexes,[5a,c−f] there was only one string compound $[Au_2Ag_2(C_6F_5)_2(CF_3CO_2)_2(PPh_2CH_2SPh)_2]$,[5a] in which the argentoaurophilic and argentophilic interactions resulted in the formation of a folded Au−Ag−Ag−Au string structure, while in the case of gold−mercury compounds, there also existed one example $\{[HgAu(CHP(S)Ph)]PF_6\}_2$, in which a bent Hg−Au−Au−Hg string structure may contain aurophilic and hydrargoaurophilic interactions.[5b] Although there are some gold string complexes with ligand-unassisted Au−Au bonds,[1g−j] the known AuAg or AuHg strings are all supported with bridging ligands.[5] In this regard, the synthesis of ligand-unsupported gold, gold−silver, and gold−mercury string complexes is still a challenge.

* To whom correspondence should be addressed. E-mail: jplang@suda.edu.cn.
† Suzhou University.
‡ Nanjing University.

10.1021/ic060655m CCC: $33.50
Published on Web 08/22/2006

Recently, we are interested in the chemistry of silver and mercury thiolate complexes, $[Ag(Tab)_2](PF_6)$ (**4**)[6a] and $[Hg(Tab)_2](PF_6)_2$ (**5**),[6b] derived from a zwitterionic thiolate $TabHPF_6$ [Tab = 4-(trimethylammonio)benzenethiolate].[7] As an extension of this study, we ran its reaction with AuI and obtained a dimeric complex $[Au(Tab)_2]_2I_2\cdot 2H_2O$ (**1**). Because **1** has low solubility in common solvents, we attempted an anion-exchange reaction of **1** with NH_4PF_6 and isolated a more soluble analogue $[Au(Tab)_2]_2(PF_6)_2$ (**2**). On the other hand, the $[Au(CN)_2]^-$ anion in $K[Au(CN)_2]$ was sometimes employed in anion-exchange reactions.[4,8b] If **2** is combined with $K[Au(CN)_2]$, the ionic interaction between the $[Au(Tab)_2]^+$ cation and the $[Au(CN)_2]^-$ anion may occur so as to form $\{[(Tab)_2Au][Au(CN)_2]\}$ species. Such species may be further assembled into certain oligomers via Au−Au aurophilic interactions. As discussed later in this paper, compound **2** exhibited luminescence in the solid state at ambient temperature and so did $K[Au(CN)_2]$[1a,2a] and its derived compounds.[8] We anticipated that when **2** reacts with $K[Au(CN)_2]$, the resulting products may modify or improve their original luminescent properties. With all of these ideas in mind, we carried out this reaction and a neutral tetranuclear gold(I) string complex $\{[(Tab)_2Au][Au(CN)_2]\}_2$ (**3**) was isolated therefrom. The isolation of **3** activated us to run analogous reactions of **4** or **5** with $K[Au(CN)_2]$, which gave rise to an expected Au/Ag metal string compound $\{[(Tab)_2Ag][Au(CN)_2]\}_2$ (**6**) and an unexpected Au/Hg complex $\{[Hg(Tab)_2][Au(CN)_2]_2\}$ (**7**). Compounds **3**, **6**, and **7** did exhibit different luminescent properties in the solid state with respect to those of their corresponding precursors. Herein, we report the syntheses, structures, and properties of **1**−**3**, **6**, and **7**.

Experimental Section

General Procedures. $TabHPF_6$ was prepared according to the literature method.[9] Other chemicals and reagents were obtained from commercial sources and used as received. All solvents were predried over activated molecular sieves and refluxed over the appropriate drying agents under argon. The IR spectra were recorded on a Nicolet MagNa-IR 550 as the KBr disk (4000−400 cm^{-1}). The elemental analyses for C, H, and N were performed on an EA1110 CHNS elemental analyzer. ^1H NMR spectra were recorded at ambient temperature on a Varian UNITY-400 spectrometer. ^1H NMR chemical shifts were referenced to the deuterated dimethyl sulfoxide (DMSO-d_6) signal. UV−vis spectra were measured on a Hitachi U-2810 spectrophotometer. The thermal analysis was performed on a Perkin-Elmer TGA-7 thermogravimetric analyzer at a heating rate of 10 °C/min and a flow rate of 100 cm^3/min (N_2). The photoluminescent spectra were performed on a Hitachi F-2500 spectrofluorometer.

Synthesis. $[Au(Tab)_2]_2I_2\cdot 2H_2O$ (1). To a suspension containing $TabHPF_6$ (0.625 g, 2 mmol) in MeOH (5 mL) was added Et_3N (2.5 mL). The resulting colorless solution was then treated with a suspension containing AuI (0.323 g, 1 mmol) in dimethylformamide

(1) (a) Forward, J. M.; Fackler, J. P., Jr.; Assefa, Z. In *Optoelectronic Properties of Inorganic Compounds*; Roundhill, D. M.; Fackler, J. P., Jr., Eds.; Plenum Press: New York, 1999; pp 195−239. (b) Omarilyn, M. O.; Jiang, F. L.; Attar, S.; Balch, A. L. *J. Am. Chem. Soc*. **2001**, *123*, 3260−3267. (c) White-Morris, R. L.; Olmstead, M. M.; Balch, A. L. *J. Am. Chem. Soc*. **2003**, *125*, 1033−1040. (d) Yang, G.; Raptis, R. G. *Inorg. Chem*. **2003**, *42*, 261−263. (e) Siemeling, U.; Robert, D.; Bruhn, C.; Fink, H.; Weidner, T.; Träger, F.; Rothenberger, A.; Fenske, D.; Priebe, A.; Maurer, J.; Winter, R. *J. Am. Chem. Soc*. **2005**, *127*, 1102−1103. (f) Yam, V. W. W.; Chan, C. L.; Li, C. K.; Wong, K. M. C. *Coord. Chem. Rev*. **2001**, *216*−*217*, 173−194. (g) Ahrland, S.; Noren, B.; Oskarsson, A. *Inorg. Chem*. **1985**, *24*, 1330−1333. (h) Conzelmann, W.; Hiller, W.; Strähle, J.; Sheldrick, G. M. *Z. Anorg. Allg. Chem*. **1984**, *512*, 169−176. (i) Adams, H. N.; Hiller, W.; Strähle, J. *Z. Anorg. Allg. Chem*. **1982**, *485*, 81−91. (j) Bauer, A.; Schmidbaur, H. *J. Am. Chem. Soc*. **1996**, *118*, 5324−5325. (k) Lee, Y. A.; McGarrah, J. E.; Lachiotte, R. J.; Eisenberg, R. *J. Am. Chem. Soc*. **2002**, *124*, 10662−10663.

(2) (a) Nagasundaram, N.; Roper, G.; Biscoe, J.; Chai, J. W.; Patterson, H. H.; Blom, N.; Ludi, A. *Inorg. Chem*. **1986**, *25*, 2947−2951. (b) Schmidbaur, H.; Graf, W.; Müller, G. *Angew. Chem., Int. Ed. Engl*. **1988**, *27*, 417−419. (c) Schmidbaur, H.; Reber, G.; Schier, A.; Wagner, F. E.; Müller, G. *Inorg. Chim. Acta* **1988**, *147*, 143−150. (d) Pathaneni, S. S.; Desiraju, G. R. *J. Chem. Soc., Dalton Trans*. **1993**, *2*, 319−323. (e) Schmidbaur, H. *Chem. Soc. Rev*. **1995**, *24*, 391−400. (f) Payne, N. C.; Ramachandran, R.; Puddephatt, R. J. *Can. J. Chem*. **1995**, *73*, 6−8. (g) Mingos, D. M. P. *J. Chem. Soc., Dalton Trans*. **1996**, *5*, 561−566. (h) Hollatz, C.; Schier, A.; Schmidbaur, H. *J. Am. Chem. Soc*. **1997**, *119*, 8115−8116. (i) Tzeng, B. C.; Chan, C. K.; Cheung, K. K.; Che, C. M.; Peng, S. M. *Chem. Commun*. **1997**, 135−136. (j) Mansour, M. A.; Connick, W. B.; Lachicotte, R. J.; Gysling, H. J.; Eisenberg, R. *J. Am. Chem. Soc*. **1998**, *120*, 1329−1330. (k) Yam, V. W. W.; Li, C. K.; Chan, C. L. *Angew. Chem., Int. Ed*. **1998**, *37*, 2857−2859. (l) Fernández, E. J.; Gimeno, M. C.; Laguna, A.; López-de-Luzuriaga, J. M.; Monge, M.; Pyykkö, P.; Sundholm, D. *J. Am. Chem. Soc*. **2000**, *122*, 7287−7293. (m) Bachman, R. E.; Fioritto, M. S.; Fetics, S. K.; Cocker, T. M. *J. Am. Chem. Soc*. **2001**, *123*, 5376−5377. (n) Lee, Y. A.; Eisenberg, R. *J. Am. Chem. Soc*. **2003**, *125*, 7778−7779. (o) Canales, S.; Crespo, O.; Gimeno, M. C.; Jones, P. G.; Laguna, A. *Inorg. Chem*. **2004**, *43*, 7234−7249. (p) Li, C. K.; Lu, X. X.; Wong, K. M. C.; Chan, C. L.; Zhu, N. Y.; Yam, V. W. W. *Inorg. Chem*. **2004**, *43*, 7421−7430. (q) Gussenboven, E. M.; Fettinger, J. C.; Pham, D. M.; Malwitz, M. M.; Balch, A. L. *J. Am. Chem. Soc*. **2005**, *127*, 10838−10839.

(3) (a) Puddephatt, R. J. In *Comprehensive Coordination Chemistry*; Wilkinson, G., Gillard, R. D., McCleverty, J. A., Eds.; Pergamon Press: Oxford, U.K., 1987; Vol. 5, pp 861−923. (b) Schmidbaur, H. *Gold Bull*. **1990**, *23*, 11−21. (c) Schmidbaur, H., Ed. *Gold: Progress in Chemistry, Biochemistry and Technology*; Wiley: New York, 1999.

(4) (a) Brandys, M. C.; Puddephatt, R. J. *Chem. Commun*. **2001**, 1280−1281. (b) Han, W.; Yi, L.; Liu, Z. Q.; Gu, W.; Yan, S. P.; Cheng, P.; Liao, D. Z.; Jiang, Z. H. *Eur. J. Inorg. Chem*. **2004**, 2130−2136. (c) Paraschiv, C.; Andruh, M.; Ferlay, S.; Hosseini, M. W.; Kyritsakas, N.; Planeix, J. M.; Stanica, N. *J. Chem. Soc., Dalton Trans*. **2005**, 1195−1202. (d) Galet, A.; Muñoz, M. C.; Martínez, V.; Real, J. A. *Chem. Commun*. **2004**, 2268−2269.

(5) (a) Fernández, E. J.; López-de-Luzuriage, J. M.; Monge, M.; Rodríguez, M. A.; Crespo, O.; Gimeno, M. C.; Laguna, A.; Jones, P. G. *Chem.*−*Eur. J*. **2000**, *6*, 636−644. (b) Wang, S. N.; Fackler, J. P., Jr. *Organometallics* **1988**, *7*, 2415−2417. (c) Mohammed, A. A.; Burini, A.; Fackler Junior, J. P. *J. Am. Chem. Soc*. **2005**, *127*, 5012−5013. (d) Wei, Q. H.; Zhang, L. Y.; Yin, G. Q.; Shi, L. X.; Chen, Z. N. *J. Am. Chem. Soc*. **2004**, *126*, 9940−9941. (e) Teo, B. K.; Zhang, H.; Shi, X. B. *J. Am. Chem. Soc*. **1993**, *115*, 8489−8490. (f) Copley, R. C. B.; Mingos, D. M. P. *J. Chem. Soc., Dalton Trans*. **1996**, 491−500.

(6) (a) Chen, J. X.; Xu, Q. F.; Zhang, Y.; Chen, Z. N.; Lang, J. P. *J. Organomet. Chem*. **2004**, *689*, 1071−1077. (b) Chen, J. X.; Zhang, W. H.; Tang, X. Y.; Ren, Z. G.; Zhang, Y.; Lang, J. P. *Inorg. Chem*. **2006**, *45*, 2568−2580.

(7) (a) Ahmed, L. S.; Clegg, W.; Davies, D. A.; Dilworth, J. R.; Elsegood, M. R. J.; Griffiths, D. V.; Horsburgh, L.; Miller, J. R.; Wheatley, N. *Polyhedron* **1998**, *18*, 593−600. (b) Zhou, C.; Raebiger, J. W.; Segal, B. M.; Holm, R. H. *Inorg. Chim. Acta* **2000**, *300*−*302*, 892−902.

(8) (a) Dunbar, K. R.; Heintz, R. A. *Prog. Inorg. Chem*. **1997**, *45*, 283−391. (b) Leznoff, D. B.; Xue, B. Y.; Batchelor, R. J.; Einstein, F. W. B.; Patrick, B. O. *Inorg. Chem*. **2001**, *40*, 6026−6034. (c) Leznoff, D. B.; Xue, B. Y.; Patrick, B. O.; Sanchez, V.; Thompson, R. C. *Chem. Commun*. **2001**, 259−260. (d) Shorrock, C. J.; Xue, B. Y.; Kim, P. B.; Batchelor, R. J.; Patrick, B. O.; Leznoff, D. B. *Inorg. Chem*. **2001**, *41*, 6743−6753. (e) Leznoff, D. B.; Xue, B. Y.; Stevens, C. L.; Storr, A.; Thompson, R. C.; Patrick, B. O. *Polyhedron* **2001**, *20*, 1247−1254. (f) Stender, M.; White-Morris, R. L.; Olmstead, M. M.; Balch, A. L. *Inorg. Chem*. **2003**, *42*, 4504−4506. (g) Stork, J. R.; Rios, D.; Pham, D.; Bicocca, V.; Olmstead, M. M.; Balch, A. L. *Inorg. Chem*. **2005**, *44*, 3466−3472.

(9) DePamphilis, B. V.; Averill, B. A.; Herskovitz, T.; Que, L., Jr.; Holm, R. H. *J. Am. Chem. Soc*. **1974**, *96*, 4159−4167.

Table 1. Crystallographic Data for **1**−**3**, **6**, and **7**

compound	**1**	**2**	**3**	**6**	**7**
molecular formula	$C_{36}H_{56}Au_2I_2N_4O_2S_4$	$C_{36}H_{52}Au_2F_{12}N_4P_2S_4$	$C_{40}H_{52}Au_4N_8S_4$	$C_{40}H_{52}Ag_2Au_2N_8S_4$	$C_{22}H_{26}Au_2HgN_6S_2$
formula weight	1352.82	1352.93	1561.00	1382.81	1033.16
cryst syst	monoclinic	monoclinic	orthorhombic	orthorhombic	monoclinic
space group	*C*2/*c*	*C*2/*c*	*Fdd*2	*Fdd*2	*C*2/*c*
size (mm^3)	0.37 × 0.25 × 0.25	0.28 × 0.25 × 0.24	0.23 × 0.23 × 0.22	0.19 × 0.16 × 0.15	0.12 × 0.12 × 0.11
a (Å)	27.775(2)	30.225(3)	18.1364(15)	18.073(2)	17.113(2)
b (Å)	9.3233(7)	8.5291(7)	32.230(3)	32.221(4)	9.9190(12)
c (Å)	18.8006(16)	20.0928(19)	15.6796(14)	15.6343(17)	15.473(2)
β (deg)	111.644(2)	121.713(2)	92.422(3)		
V ($Å^3$)	4525.2(6)	4406.4(7)	9165.3(14)	9104.3(18)	2624.0(6)
Z	4	4	8	8	4
T (K)	193	193	193	193	193
D_{calc} (g cm^{-3})	1.986	2.039	2.263	2.018	2.615
λ(Mo Kα) (Å)	0.710 70	0.710 70	0.710 70	0.710 70	0.710 70
μ (cm^{-1})	80.60	69.98	129.86	74.95	171.72
$2\theta_{max}$ (deg)	55.0	55.0	55.0	50.6	55.0
no. of reflns collected	24385	23586	25257	21970	14188
no. of unique reflns	5171 (R_{int} = 0.0877)	5020 (R_{int} = 0.0372)	5233(R_{int} = 0.0488)	4011(R_{int} = 0.0278)	2992(R_{int}= 0.0350)
no. of observed reflns	4412 [$I > 2.00\sigma(I)$]	4745 [$I > 2.00\sigma(I)$]	4047 [$I > 2.00\sigma(I)$]	3454 [$I > 2.00\sigma(I)$]	2732 [$I > 2.00\sigma(I)$]
no. of param	234	279	232	244	155
R^a	0.0374	0.0277	0.0380	0.0248	0.0295
wR^b	0.0805	0.0658	0.0776	0.0569	0.0708
GOF[c]	1.008	1.133	1.146	1.080	0.953
largest residual peaks, holes (e $Å^{-3}$)	0.872, −0.825	0.884, −0.697	0.983, −0.904	1.176, −0.887	0.971, −0.974

[a] $R = \sum||F_o| - |F_c||/\sum|F_o|$. [b] $wR = \{\sum w(F_o^2 - F_c^2)^2/\sum w(F_o^2)^2\}^{1/2}$. [c] GOF = $\{\sum w((F_o^2 - F_c^2)^2)/(n - p)\}^{1/2}$, where n = number of reflections and p = total numbers of parameters refined.

(DMF; 5 mL). The mixture was stirred for 0.5 h to dissolve the AuI solid and then filtered. Slow evaporation of the solvents from the filtrate in air at room temperature led to the formation of colorless prisms of **1**, which were collected by filtration, washed with Et_2O, and dried in vacuo. Yield: 0.588 g (87.0% based on AuI). Anal. Calcd for $C_{36}H_{56}Au_2I_2N_4O_2S_4$: C, 31.96; H, 4.17; N, 4.14. Found: C, 31.84; H, 4.28; N, 4.35. IR (KBr disk): 1580 (w), 1484 (m), 1407 (w), 1120 (w), 1010 (w), 949 (m), 817 (s), 744 (w), 547 (m) cm^{-1}. UV−vis [DMF; λ_{max}, nm (ϵ, M^{-1} cm^{-1})]: 304 (175 800). ^{1}H NMR (400 MHz, DMSO-d_6): δ 7.53−7.65 (m, 4H, Ph), 3.51 (s, 9H, NMe_3).

[Au(Tab)$_2$]$_2$(PF$_6$)$_2$ (2). To a suspension of **1** (0.675 g, 0.5 mmol) in DMF (5 mL) was added NH_4PF_6 (0.163 g, 1 mmol). The resulting mixture was stirred for 1 h to form a colorless solution and filtered. Diethyl ether (20 mL) was layered onto the filtrate to form colorless prisms of **2** in several days, which were collected by filtration, washed with Et_2O, and dried in vacuo. Yield: 0.663 g (98.0% based on **1**). Anal. Calcd for $C_{36}H_{52}Au_2F_{12}N_4P_2S_4$: C, 31.96; H, 3.87; N, 4.14. Found: C, 32.25; H, 3.42; N, 3.93. IR (KBr disk): 1581 (w), 1485 (m), 1408 (w), 1122 (w), 1006 (w), 960 (m), 841 (s), 744 (w), 559 (m) cm^{-1}. UV−vis [DMF; λ_{max}, nm (ϵ, M^{-1} cm^{-1})]: 304 (263 800). ^{1}H NMR (400 MHz, DMSO-d_6): δ 7.51−7.63 (m, 4H, Ph), 3.50 (s, 9H, NMe_3).

{**[(Tab)$_2$Au][Au(CN)$_2$]**}$_2$ **(3).** To a solution containing **2** (0.676 g, 0.5 mmol) in DMF (5 mL) was added a solution of K[Au(CN)$_2$] (0.288 g, 1 mmol) in MeOH (5 mL). The mixture was stirred for 5 min and then filtered to give a clear colorless solution. Layering diethyl ether (20 mL) onto the filtrate formed block colorless crystals of **3**, which were collected by filtration, washed with MeOH/Et_2O (1:4), and dried in vacuo. Yield: 0.749 g (96.0% based on **2**). Anal. Calcd for $C_{40}H_{52}Au_4N_8S_4$: C, 30.78; H, 3.36; N, 7.18. Found: C, 30.52; H, 3.23; N, 7.43. IR (KBr disk): 2156 (w), 2137 (s), 1577 (m), 1485 (s), 1404 (s), 1234 (w), 1122 (s), 1010 (s), 952 (s), 837 (m), 744 (m), 551 (m) cm^{-1}. UV−vis [DMF; λ_{max}, nm (ϵ, M^{-1} cm^{-1})]: 302 (163 600). ^{1}H NMR (400 MHz, DMSO-d_6): δ 7.54−7.63 (m, 4H, Ph), 3.51 (s, 9H, NMe_3).

{**[(Tab)$_2$Ag][Au(CN)$_2$]**}$_2$ **(6).** To a solution containing **4** (0.587 g, 1 mmol) in DMF (5 mL) was added a solution of K[Au(CN)$_2$] (0.288 g, 1 mmol) in MeOH (5 mL). A workup similar to that used in the isolation of **3** afforded colorless prisms of **6**. Yield: 0.657 g (95.0% based on **4**). Anal. Calcd for $C_{40}H_{52}Ag_2Au_2N_8S_4$: C, 34.74; H, 3.79; N, 8.10. Found: C, 34.32; H, 3.53; N, 8.44. IR (KBr disk): 2156 (w), 2133 (s), 1576 (m), 1485 (s), 1408 (s), 1234 (w), 1122 (s), 1010 (s), 952 (s), 837 (m), 744 (m), 551 (m) cm^{-1}. UV−vis [DMF; λ_{max}, nm (ϵ, M^{-1} cm^{-1})]: 296 (308 700). ^{1}H NMR (400 MHz, DMSO-d_6): δ 7.54−7.66 (m, 4H, Ph), 3.52 (s, 9H, NMe_3).

{**[Hg(Tab)$_2$][Au(CN)$_2$]$_2$**} **(7).** To a solution containing **5** (0.824 g, 1 mmol) in DMF (5 mL) was added a solution of K[Au(CN)$_2$] (0.576 g, 2 mmol) in MeOH (5 mL). A workup similar to that used in the isolation of **3** produced colorless prisms of **7**. Yield: 0.961 g (93.0% based on **5**). Anal. Calcd for $C_{22}H_{26}Au_2HgN_6S_2$: C, 25.58; H, 2.54; N, 8.13. Found: C, 25.41; H, 2.34; N, 8.59. IR (KBr disk): 2156 (w), 2137 (s), 1581 (m), 1489 (s), 1404 (s), 1230 (w), 1126 (s), 1010 (s), 949 (s), 817 (m), 744 (m), 547 (m), 424 (m) cm^{-1}. UV−vis [DMF; λ_{max}, nm (ϵ, M^{-1} cm^{-1})]: 276 (276 600). ^{1}H NMR (400 MHz, DMSO-d_6): δ 7.59−7.74 (m, 4H, Ph), 3.51 (s, 9H, NMe_3).

X-ray Structure Determination. X-ray-quality crystals of **1**−**3**, **6**, and **7** were obtained directly from the above preparations. All measurements were made on a Rigaku Mercury CCD X-ray diffractometer by using graphite-monochromated Mo Kα (λ = 0.710 70 Å). Crystals of **1**−**3**, **6**, and **7** were mounted with grease at the top of a glass fiber and cooled at 193 K in a liquid-N_2 stream. Cell parameters were refined by using the program *CrystalClear* (Rigaku and MSC, version 1.3, 2001). The collected data were

Scheme 1

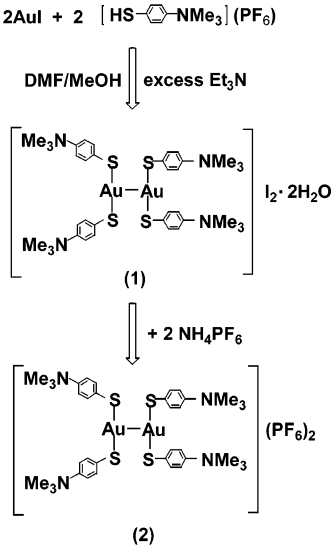

reduced by using the program *CrystalStructure* (Rigaku and MSC, version 3.60, 2004) while an absorption correction (multiscan) was applied.

The crystal structures of **1**−**3**, **6**, and **7** were solved by direct methods and refined on F^2 by full-matrix least-squares methods with the *SHELXTL-97* program.[10] All non-H atoms were refined anisotropically. The H atoms of the solvated water molecule in **1** were located from the Fourier maps, and all of the other H atoms were placed in geometrically idealized positions (C−H = 0.98 Å for methyl groups; C−H = 0.95 Å for phenyl groups) and constrained to ride on their parent atoms with $U_{iso}(H) = 1.2U_{eq}(C)$ for phenyl groups and $U_{iso}(H) = 1.5U_{eq}(C)$ for methyl groups. A summary of the key crystallographic information for **1**−**3**, **6**, and **7** was tabulated in Table 1.

Results and Discussion

Synthesis. The reaction of AuI with 2 equiv of $TabHPF_6$ under excess Et_3N in MeOH/DMF resulted in a colorless solution. Slow evaporation of solvents from the solution led to the formation of colorless prisms of **1** in 87.0% yield (Scheme 1). The existence of two solvated water molecules in **1** may be attributed to the fact that excess Et_3N readily absorbs water from air. Compound **1** is slightly soluble in DMF and DMSO and almost insoluble in common solvents such as MeOH, MeCN, and CH_2Cl_2. Because of its poor solubility, we attempted exchange of the iodides of **1** with larger anions. The reaction of **1** with 2 equiv of NH_4PF_6 produced its analogue **2** in an almost quantitative yield. **2** was readily soluble in common solvents such as MeCN, DMF, and DMSO and may be a suitable precursor for the further assembly reaction. As shown in Scheme 2, treatment of **2** with 2 equiv of $K[Au(CN)_2]$ followed by a standard workup gave rise to a neutral tetranuclear gold(I) string complex **3** in 96% yield. A similar reaction of **4** with equimolar $K[Au(CN)_2]$ afforded a Au/Ag string analogue **6** in 95% yield. However, analogous reaction of **5** with 2 equiv of $K[Au(CN)_2]$ did not yield our expected Au/Hg string complex $\{[(Tab)_2Hg][Au(CN)_2]\}_2(PF_6)_2$ but generated complex **7** in 93% yield (Scheme 3). As described later in this paper, the failed formation of the Au/Hg string complex may be ascribed to the fact that the hydrargoaurophilic interaction is weaker than the aurophilic and argentoaurophilic interactions and even the secondary Hg···N interactions.

Scheme 2

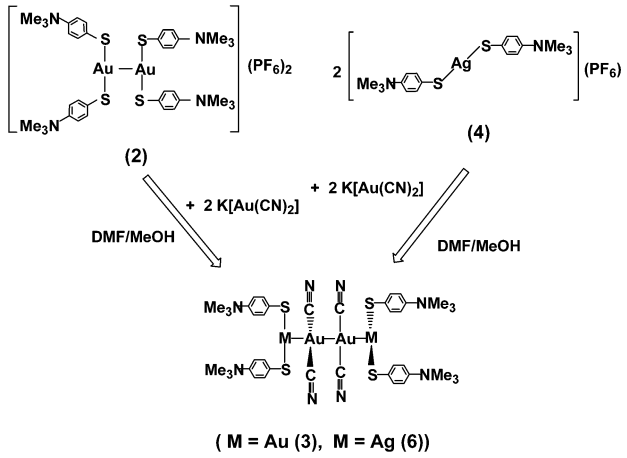

Scheme 3

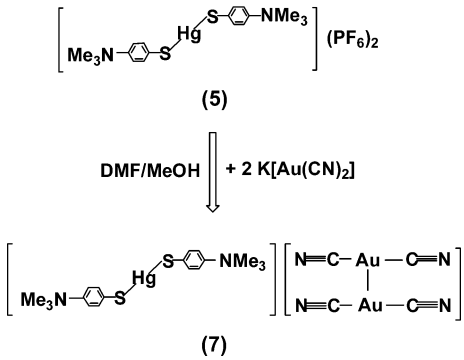

Crystal Structures of 1 and 2. Both **1** and **2** crystallize in the monoclinic space group *C2/c*, and the asymmetric unit of **1** consists of half of the $[Au(Tab)_2]_2^{2+}$ dication, one I^- anion, and one solvated water molecule, while that of **2** has half of the $[Au(Tab)_2]_2^{2+}$ dication and one PF_6^- anion. Because the structures of the dications of **1** and **2** are similar, only the perspective view of the dication of **1** is depicted in Figure 1. Selected bond lengths and angles for **1** and **2** are compared in Table 2. The $[Au(Tab)_2]_2^{2+}$ dication of **1** or **2** consists of two $[Au(Tab)_2]^+$ cations that are linked via one aurophilic Au−Au bonding interaction, forming a ligand-unassisted dimeric structure with an inversion center lying on the midpoint of the Au1···Au2 line and a crystallographic 2-fold axis running along the line of the Au1 and Au2 atoms. Such a dimeric structure resembles those of other diauro(I) complexes such as $[Au(2\text{-}Pys)(PPh_2PyH)]_2(PF_6)_2 \cdot CH_2Cl_2 \cdot 2H_2O$ (PySH = 2-mercaptopyridine),[11a] $[AuCl(dppa)]_2$ (dppa = diphenylphosphinous acid),[11b] $[AuCl(tfdppp)]_2(PF_6)_2 \cdot 0.5CH_2Cl_2$ (tfdppp = 1,1,2-trifluoro-3,3-diphenyl-3-phosphaprop-

(10) Sheldrick, G. M. *SHELX-97 and SHELXL-97, Program for Crystal Structure Refinement*; University of Göttingen: Göttingen, Germany, 1997.

(11) (a) Hao, L. J.; Mansour, M. A.; Lachicotte, R. J.; Gysling, H. J.; Eisenberg, R. *Inorg. Chem.* **2000**, *39*, 5520−5529. (b) Hollatz, C.; Schier, A.; Riede, J.; Schimidbaur, H. *J. Chem. Soc., Dalton Trans.* **1999**, 111−114. (c) Banger, K. K.; Banhaun, R. P.; Brisdon, A. K.;

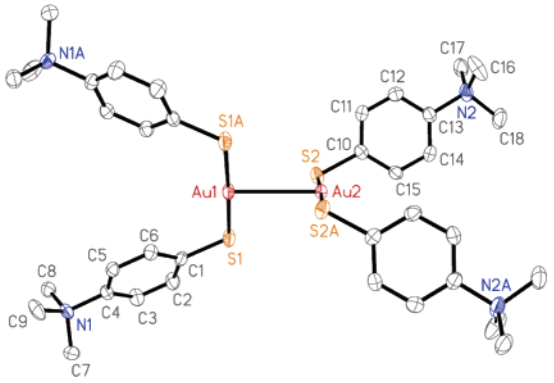

Figure 1. Perspective view of the $[Au(Tab)_2]_2^{2+}$ dimer of **1** with 50% thermal ellipsoids. All H atoms are omitted for clarity. Symmetry transformations used to generate equivalent atoms: A, $-x + 1, y, -z + {}^1/_2$.

Table 2. Selected Bond Distances (Å) and Angles (deg) for **1** and **2**

	1	**2**
Au1−S1	2.2950(13)	2.3032(9)
Au2−S2	2.3055(13)	2.3046(9)
Au1−Au2	3.0184(4)	3.0146(3)
S1−Au1−S1A	177.81(6)	177.41(5)
S2−Au2−S2	177.73(6)	175.02(5)

1-en-3-yl),[11c] and [AuCl(*o*-xylylisocyano)]$_2$.[11d] In the structure of **1** or **2**, the Au−Au bond length, 3.0184(4) Å for **1** or 3.0146(3) Å for **2**, is shorter than those found in [AuCl(dppa)]$_2$ [3.111(2) Å], [AuCl(tfdppp)]$_2(PF_6)_2$·0.5CH_2Cl_2 [3.194(3) Å], and [AuCl(*o*-xylylisocyano)]$_2$ [3.357(4) Å].

In each $[Au(Tab)_2]^+$ cation of **1** or **2**, the Au atom is strongly coordinated by two S atoms of the two Tab moieties, forming an approximate linear AuS_2 coordination geometry [$(S-Au-S)_{av}$ = 177.77(6)° for **1** and 176.22(6)° for **2**]. The S1−Au1−S1A and S2−Au2−S2A lines are not parallel but are twisted by 56.9° for **1** and 56.6° for **2**. The two $^-SC_6H_4NMe_3^+$ groups in **4** or **5** are directed at opposite directions. However, each cation in **1** or **2** has its two $^-SC_6H_4NMe_3^+$ groups oriented in the same direction. The dihedral angles between the two phenyl groups in each $[Au(Tab)_2]^+$ cation are quite different: 11.6° vs 40.2° for **1** and 6.6° vs 38.7° for **2**. The mean Au−S bond lengths, 2.300(13) Å for **1** and 2.304(9) Å for **2**, are between $[Au(tmtat)_2](BF_4)$ [2.272(4) Å; tmtat = bis(1,4,5-trimethyl-1,2,4-triazolium-3-thiolate)][12a] and [Au(Hdamp-C^1)(HSthiaz)$_2$]Cl_2 [2.329(3) Å; Hdamp = 2-[(dimethylamino)methyl]phenyl-C^1, HSthiaz = 2-mercapto-1,3-thiazoline].[12b]

The dications in the crystals of **1** or **2** are parallel to each other. The solvated water molecules and iodides in **1** or the associated $[PF_6]^-$ anions in **2** are positioned between these parallel dications. The separations between two neighboring cations are 13.89 Å (**1**) vs 15. 11 Å (**2**) (along the *a* axis), 6.30 Å (**1**) vs 14.04 Å (**2**) (along the *b* axis), and 9.40 Å (**1**) vs 10.04 Å (**2**) (along the *c* axis), respectively. It is noted that **1** and **2** have very different hydrogen-bound structures in their crystals. For **1**, the iodide interacts with the solvated water molecule to afford one intramolecular hydrogen bond and one intermolecular hydrogen bond [O1···I1 ($-x + {}^3/_2$, $y + -{}^1/_2$, $-z + {}^1/_2$)]. The O atom of the solvated water molecule also interacts with the H atoms of the phenyl groups to afford two intermolecular hydrogen bonds [C7···O1 ($-x + 1, y, -z + {}^1/_2$); C12···O1 ($-x + {}^3/_2, y + {}^3/_2, -z + {}^1/_2$)], forming a 2D network extending along the *ab* plane (Figure 2).

In the case of **2**, the hydrogen-bonding interactions are rather complicated. The F atoms of the PF_6^- anion interacts with the H atoms of the methyl group or the phenyl group to afford one intramolecular hydrogen bond [C16···F1] and five intermolecular hydrogen bonds [C7···F2 ($x, 2 - y, z + {}^1/_2$); C7···F4 ($-x + {}^3/_2, y + {}^3/_2, -z + {}^1/_2$), C18···F5 ($x, y - 1, z$); C5···F6 ($-x + {}^3/_2, y + {}^1/_2, -z + {}^1/_2$), C8···F6 ($x, 2 - y, z + {}^1/_2$)], forming a 3D hydrogen-bound structure (Figure 3).

Crystal Structures of 3 and 6. Both **3** and **6** crystallize in the orthorhombic space group *Fdd*2, and the asymmetric unit consists of half of the $\{[(Tab)_2M][Au(CN)_2]\}_2$ (M = Au and Ag) molecule. **3** and **6** are isotypic, and their cell parameters are essentially identical, as are their molecular structures. Therefore, only the perspective view of **3** is presented in Figure 4. The bond lengths and angles for **3** and **6** are compared in Table 3. In the structures of **3** and **6**, each of the two pairs of the $[M(Tab)_2]^+$ cation and the $[Au(CN)_2]^-$ anion are held together via ionic interaction between the $[Au(Tab)_2]^+$ cation and the $[Au(CN)_2]^-$ anion to form a $\{[(Tab)_2M][Au(CN)_2]\}$ species. Two such species are further connected by one Au−Au aurophilic bonding interaction to form an interesting Au_4 or Ag_2Au_2 string structure with three ligand-unassisted Au−Au or Au−Ag bonds. There is a crystallographic 2-fold axis running along the Au_4 or Ag_2Au_2 string. The torsion angle for Au3···Au1···Au2···Au4 in **3** or Ag1···Au1···Au2···Ag2 in **6** is 0°. The length of the Au_4 or Ag_2Au_2 string is 9.124 Å for **3** or 8.892 Å for **6**. The linear Au_4 structure of **3** resembles those observed in $[X_2AuAu(Py)_2]_2$ (X = Cl, Br, and I).[1h,i] However, the Ag_2Au_2 linear structure of **6** is different from those of the known Ag_2Au_2 compounds, which usually consist of a highly bent or zigzag Ag_2Au_2 core structure.[5c−f]

The four $^-SC_6H_4NMe_3^+$ and four CN^- groups covering the string of **3** and **6** are staggered to minimize their steric hindrance. For **3**, the two $^-SC_6H_4NMe_3^+$ groups in each $[Au(Tab)_2]^+$ cation are oriented in the same direction, and the dihedral angles between two phenyl rings in each $[Au(Tab)_2]^+$ cation are 14.0° and 53.6°, which are larger than the corresponding values in **1** and **2**. The two S−Au−S lines are twisted by 47.9°, which is slightly smaller than those in **1** and **2**. In the two $[Au(Tab)_2]^+$ cations of **3**, the mean Au−S distance [2.314(3) Å] is comparable to those of **1** and **2** while the mean S−Au−S angle (173.86°) is smaller than those of **1** and **2**. On the other hand, it is noted that the two $^-SC_6H_4NMe_3^+$ groups in each $[Ag(Tab)_2]$ unit of **6** are oriented in the same direction, which is different from that

Cross, W. I.; Damant, G.; Parsons, S.; Pritchard, R. G.; Sousa-Pedrares, A. *J. Chem. Soc., Dalton Trans.* **1999**, 427−434. (d) Echen, H.; Olmstead, M. M.; Noll, B. C.; Attar, S.; Schlyer, B.; Balch, A. L. *J. Chem. Soc., Dalton Trans.* **1998**, 3715−3720.

(12) (a) Deaton, J. C.; Luss, H. R. *J. Chem. Soc., Dalton Trans.* **1999**, *18*, 3163−3167. (b) Abram, U. J.; Ortner, M. K.; Müller, M. *J. Chem. Soc., Dalton Trans.* **1998**, *6*, 1011−1019.

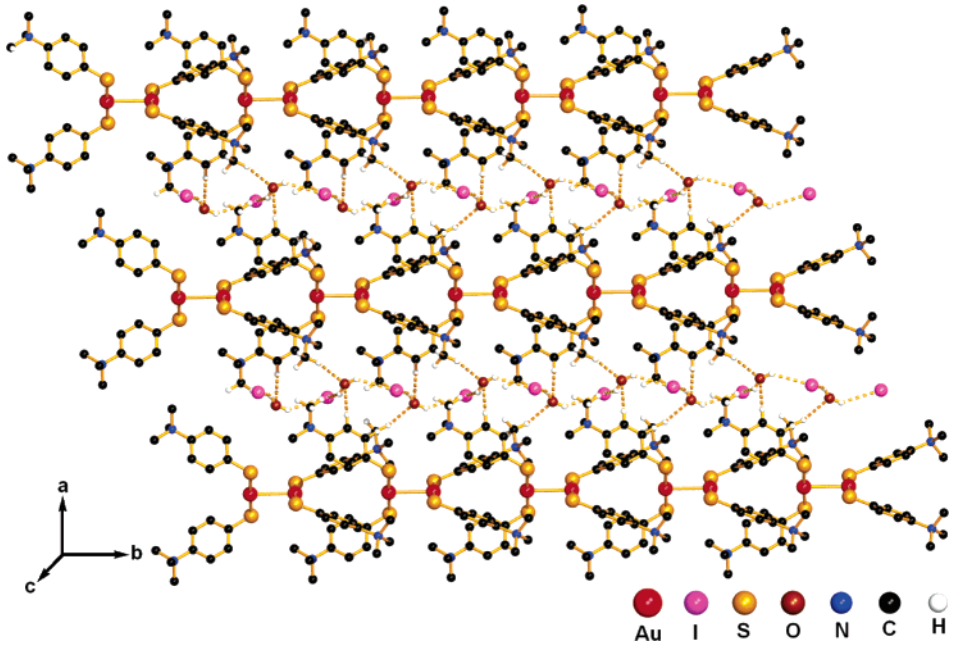

Figure 2. 2D network formed via hydrogen-bonding interactions in **1** (extended along the *ab* plane). All H atoms except those related to hydrogen-bonding interactions are omitted for clarity.

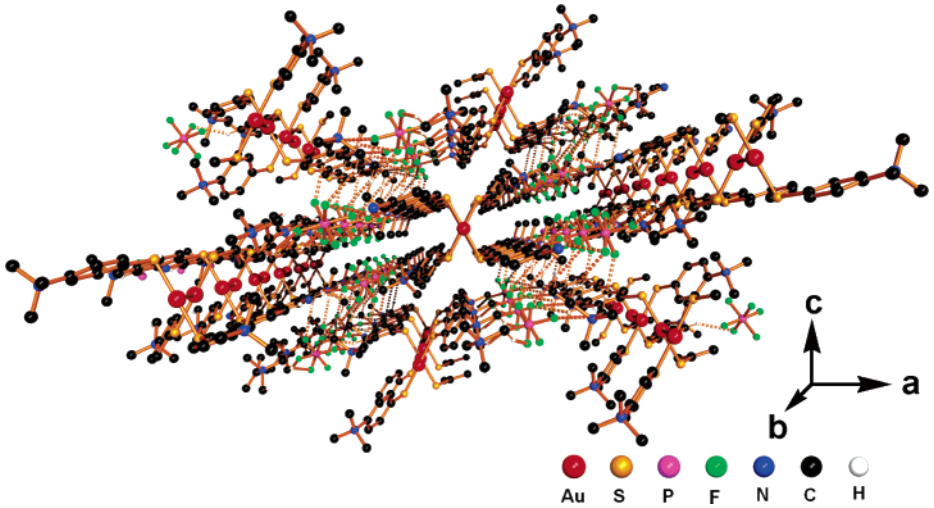

Figure 3. 3D structure formed via hydrogen-bonding interactions in **2** looking down the *b* axis. All H atoms except those related to hydrogen-bonding interactions are omitted for clarity.

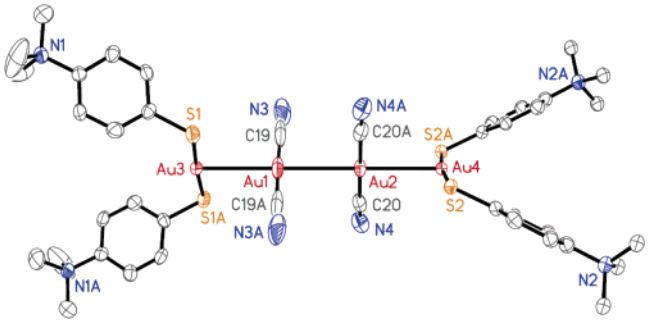

Figure 4. Perspective view of the molecular structure of **3** with 50% thermal ellipsoids. All H atoms are omitted for clarity. Symmetry transformations used to generate equivalent atoms: A, $-x + 1/2, -y + 1/2, z$.

of its precursor **4**, implying that one of the two $^{-}SC_6H_4NMe_3^{+}$ groups of **4** was rotated along the S−Ag−S line by 180° during the reaction. The two S−Ag−S lines from two [Ag(Tab)$_2$] units in **6** are twisted by 47.2°, which is much smaller than that in **4** (91.1°). The mean Ag−S distance [2.382(15) Å] of **6** is almost the same as that of **4** [2.385(5) Å], while the average S−Ag−S angle of **6** [171.46(3)°] is smaller than that of **4** [178.29(8)°]. The dihedral angles between the two phenyl rings in each [Ag(Tab)$_2$] unit in **6** are 12.8° and 54.2°, respectively.

In the [Au(CN)$_2$]$_2$ part of **3** or **6**, the Au1−Au2 bond length [3.0688(6) Å (**3**) or 3.0140(5) Å (**6**)] is shorter than those of Tb[Au(CN)$_2$]$_3$·3H$_2$O [3.31(1) Å],[13] [C$_{36}$H$_{48}$N$_{18}$][Au$_4$(CN)$_8$]$_2$(NO$_3$)$_2$·2H$_2$O [3.344(2) Å; C$_{36}$H$_{48}$N$_{18}$ = 6,12,18,24,30,36-hexaamino-4,10,16,22,28,34-hexamethylcalix(6)pyrimidinium),[14] Cs$_2$Na[Au(CN)$_2$]$_3$ [3.448(1)−3.620(1) Å],[15]

(13) Tanner, P. A.; Zhou, X. J.; Wong, W. T.; Kratzer, C.; Yersin, H. *J. Phys. Chem. B* **2005**, *109*, 13083−13090.

Table 3. Selected Bond Distances (Å) and Angles (deg) for **3**, **6**, and **7**

	Compound **3**		
Au3−S1	2.316(2)	Au4−S2	2.312(3)
Au1−C19	1.91(2)	Au2−C20	1.977(11)
Au3−Au1	3.0311(11)	Au4−Au2	3.0239(9)
Au1−Au2	3.0688(6)		
S1−Au3−S1A	175.91(12)	S2−Au4-S2A	171.78(10)
C19−Au1−C19A	177.6(7)	C20−Au2−C20A	179.7(5)
Au3−Au1−Au2	180.0	Au4−Au2−Au1	180.0
	Compound **6**		
Au1−S1	2.3841(15)	Ag2−S2	2.3788(16),
Au1−C19	1.981(10)	Au2−C20	1.989(7)
Ag1−Au1	2.9598(7)	Ag2−Au2	2.9185(7)
Au1−Au2	3.0140(5)		
S1−Ag1−S1A	177.36(8)	S2−Ag2−S2A	165.55(8)
C19−Au1−C19A	179.7(4)	C20−Au2−C20A	178.1(3)
Ag1−Au1−Au2	180.0	Ag2−Au2−Au1	180.0
	Compound **7**		
Hg1−S1	2.3369(15)	Au1−C10	1.979(7)
Au1−C11	1.990(6)	Au1−Au1A	3.2619(7)
Hg1···N3B	3.1434(7)		
S1−Hg1−S1A	180.0	N3B−Hg1−N3D	180.00
S1−Hg1−N3B	109.46(5)	S1−Hg1−N3D	70.53(4)
C10−Au1−C11	175.3(3)		

and $K[Au(CN)]_2$ [3.64(3) Å].[16] The mean Au−Au contact [3.0412(9) Å] of **3** is slightly longer than those of **1** or **2**. The mean Ag−Au contact [2.9391(7) Å] of **6** is slightly longer than that of $[AgAu(mtp)_2]$ [2.9124(13) Å; mtp = diphenylmethylenethiophosphinate].[17] In addition, the mean Au−C bond length and C−Au−C angle are 1.94(6) Å and 178.65(8)° for **3** and 1.99(8) Å and 178.9(4)° for **6**. The twisted angle (90.7°) for the two C≡N−Au−C≡N lines of **3** is similar to that of **6** (91.7°).

In the crystals of **3** and **6**, the string molecules are parallel to each other along the *c* axis and there are no additional aurophilic bonds between the nearest molecules (see the Supporting Information). It is noted that **3** or **6** contains some nonconventional C−H···Au(Ag) hydrogen-bonding interactions.[18] For **3**, Au3 interacts the H atoms of the methyl group to afford one intermolecular bond C16 [$x, y, z - 1$], forming a 1D chain structure extending along the *c* axis. The hydrogen-bonding interaction between Ag1 and the H atoms of the methyl group with C18 [$x, y, -1 + z$] in **6** also forms a similar 1D chain structure (see the Supporting Information). The N atoms of cyanides or the S atoms of Tab ligands in **3** interact with the H atoms of the methyl groups or phenyl groups of the neighboring chains [C16···N4 ($x + {}^1/_4, -y + {}^3/_4, -z - {}^3/_4$), C18···N4 ($x + {}^1/_2, y, z + {}^1/_2$); C5···S2 ($x, y, z - 1$), and C7···S2 ($-x + {}^3/_4, y - {}^1/_4, -z - {}^3/_4$)] to afford four intermolecular hydrogen bonds, thereby forming an interesting 3D hydrogen-bound structure (Figure 5). In the case of **6**, lots of intermolecular hydrogen bonds formed from interactions of the N atoms of cyanides or the S atoms of Tab ligands with the methyl groups or phenyl groups of the neighboring chains afford a more complicated 3D hydrogen-bound structure (see the Supporting Information).

Crystal Structure of 7. Compound **7** crystallizes in the monoclinic space group *C*2/*c*, and the asymmetric unit consists of half of the $[Hg(Tab)_2]^{2+}$ dication and half of the $[Au(CN)_2]_2^{2-}$ anion. The $[Hg(Tab)_2]^{2+}$ dications are parallel to each other, and the Hg···Hg separation between two neighboring cations is ca. 9.89 Å, whereas each $[Au(CN)_2]_2^{2-}$ dianion is positioned between the dications, and thus two N atoms from the cyanides of the two neighboring $[Au(CN)_2]_2^{2-}$ dianions have secondary interactions with the Hg1 atom, forming a 1D chain structure extending along the [101] plane (Figure 6). The Hg1 center may be viewed as having a pseudo-square-planar coordination geometry. The Hg1···N3B contact is 3.1434(7) Å (Table 3), which is shorter than the sum of the van der Waals radii of nitrogen (1.55 Å)[19a] and mercury (1.73 Å).[19b] There is an inversion center lying on the midpoint of the Hg1 atom and a crystallographic 2-fold axis running through the Hg1 atom of **7**.

The structure of the dication of **7** retains the same structure as its precursor **5** because their Hg−S bond lengths and S−Hg−S bond angles are almost identical. An analogues dimeric $[Au(CN)_2]_2^{2-}$ dianion is again formed from one Au1−Au1A aurophilic interaction [3.2619(7) Å], which is weaker than those found in **3** and **6**. The two linear C≡N−Au−C≡N lines are twisted by 51.3°, which is 39−40° smaller than those of the corresponding values in **3** and **6**. The average Au−C bond length and C−Au−C bond angle are 1.9845(6) Å and 175.3(3)°, which are close to the corresponding values in **3** and **6**.

In the crystal of **7**, there is one hydrogen-bonding interaction between N2 and the methyl group with C9 [$-x, y, -z + {}^1/_2$]. Four such symmetrically related hydrogen bonds interconnect $[Hg(Tab)_2][Au(CN)_2]_2$ species into a 2D network (see the Supporting Information). Such 2D layers are further linked by the Au−Au aurophilic interactions [3.2619(7) Å] and hydrogen-bonding interactions between S1 and the methyl group with C8 [$-x, -y + 1, -z + 1$] along the *c* axis, forming a 3D structure (Figure 7).

Thermal Properties of 1−3, 6, and 7. The thermogravimetric analysis revealed that pure Tab decomposed at the range of 169−400 °C. Compound **1** underwent decomposition at two stages within 46−500 °C. The first stage has a weight loss of 2.65% in the region of 46−110 °C, which corresponds to the loss of two H_2O solvated molecules (calcd 2.66%). The second weight loss of 67.78% in the region of 150−450 °C roughly corresponds to the loss of I and Tab ligands (calcd 68.22%). Compound **2** became decomposed at 182 °C. The whole weight loss in **2** is 71.50%, which corresponds to the loss of Tab and PF_6^- (calcd 70.89%). **3** and **6** underwent decomposition at two stages. Because the

(14) Cramer, R. E.; Smith, D. W.; Van Doorne, W. *Inorg. Chem.* **1998**, *37*, 5895−5901.
(15) Blom, N.; Ludi, A. *Acta Crystallogr.* **1984**, *C40*, 1770−1772.
(16) Rosenzweig, A.; Cromer, D. T. *Acta Crystallogr.* **1959**, *12*, 709−712.
(17) Rawashdeh-Omary, M. A.; Omary, M. A.; Fackler, J. P., Jr. *Inorg. Chim. Acta* **2002**, *334*, 376−384.
(18) (a) Kryachko, E. S.; Remacle, F. *Nano Lett.* **2005**, *5*, 735−739. (b) Kryachko, E. S.; Karpfen, A.; Remacle, F. *J. Phys. Chem.* **2005**, *109*, 7309−7318. (c) Zhang, G. Q.; Yang, G. Q.; Chen, Q. Q.; Ma, J. S. *Cryst. Growth Des.* **2005**, *5*, 661−666.
(19) (a) Bondi, A. *J. Phys. Chem.* **1964**, *68*, 441−451. (b) Canty, A. J.; Deacon, G. B. *Inorg. Chim. Acta* **1980**, *45*, 225−230.

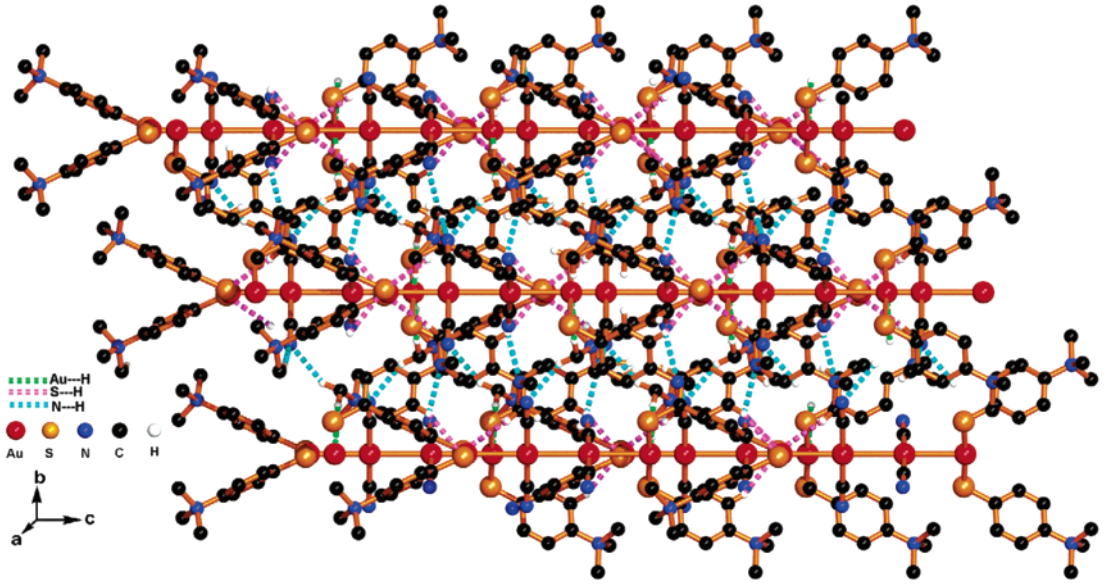

Figure 5. 3D hydrogen-bound structure formed via hydrogen-bonding interactions in **3** looking along the *a* axis. All H atoms except those related to hydrogen-bonding interactions are omitted for clarity.

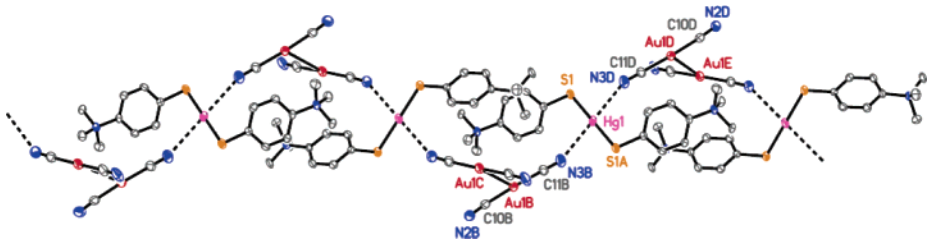

Figure 6. 1D chain (extended along [101]) formed via Hg···N secondary interactions in **7** with 50% thermal ellipsoids. All H atoms are omitted for clarity. Symmetry transformations used to generate equivalent atoms: A, $-x + {}^1/_2, -y + {}^3/_2, -z + 1$; B, $-x + 1, -y + 1, -z + 1$; C, $x, -y + 1, z + {}^1/_2$; D, $x - {}^1/_2, y + {}^1/_2, z$; E, $-x + {}^1/_2, y + {}^1/_2, -z + {}^1/_2$.

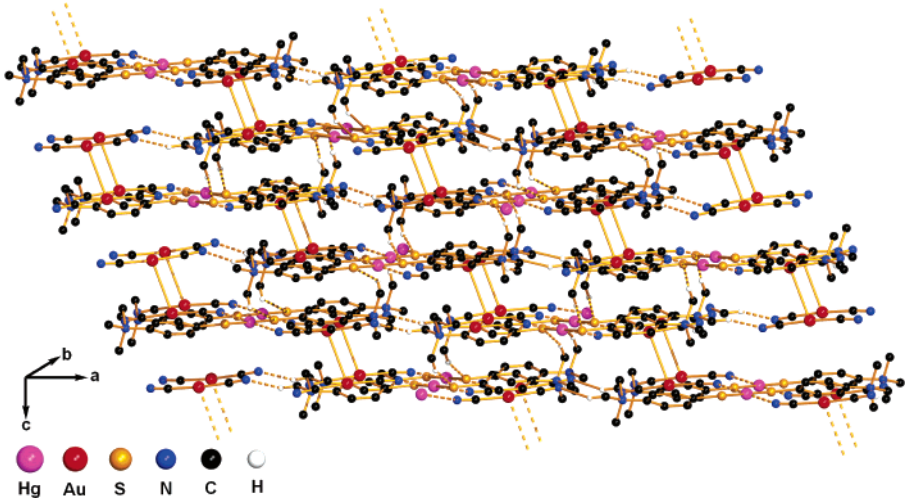

Figure 7. 3D structure of **7** looking along the *b* axis. All H atoms except those related to hydrogen-bonding interactions are omitted for clarity.

coordinated CN^- anions in **3** or **6** may be released as $(CN)_2$[20] at a temperature overlapped with the decomposition temperature of coordinated Tab ligand, the total weight losses for **3** between 255 and 468 °C and for **6** between 191 and 290 °C are 49.09% and 55.51%, respectively, which corresponds to the combined loss of Tab and CN (calcd 49.53% for **3** and 55.91% for **6**). In the thermogram of **7**, only one stage occurs around 250 °C. Because of the sublimation of the mercury thiolate compound in **7**,[8a,21] the whole weight loss in **7** is 61.16%, which corresponds to the loss of Hg(Tab)$_2$ and cyanides (calcd 61.87%). Visual inspection and X-ray fluorescence analysis revealed that the residue after thermolysis was essentially metal. The remaining weights of **1**−**3** and **7** are 29.57%, 28.50%, 50.91%, and 38.84%,

(20) Lefebvre, J.; Batchelor, R. J.; Leznoff, D. B. *J. Am. Chem. Soc.* **2004**, *126*, 16117−16125.

(21) Bharara, M. S.; Bui, T. H.; Parkin, S.; Atwood, D. A. *Inorg. Chem.* **2005**, *44*, 5753−5760.

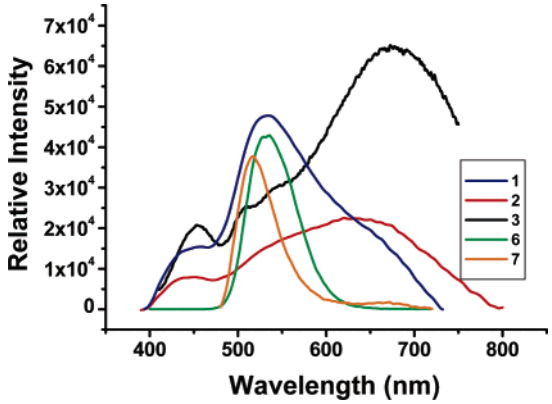

Figure 8. Emission spectra of **1**−**3**, **6**, and **7** in the solid state at ambient temperature.

which correspond to the pure Au (calcd 29.12% for **1**, 29.11% for **2**, 50.47% for **3**, and 38.13% for **7**), while the remaining weight of **6** is 44.49%, which corresponds to the mixed metals of AgAu (calcd 44.09%; see the Supporting Information).

Spectral Aspects of 1−3, 6, and 7. Solids **1**−**3**, **6**, and **7** are relatively stable toward oxygen and moisture. Compound **1** is slightly soluble in DMF and DMSO, while **2**, **3**, **6**, and **7** are soluble in DMSO and DMF. The elemental analyses of **1**−**3**, **6**, and **7** were consistent with their chemical formulas. The IR spectrum of **2** showed the characteristic P−F stretching vibrations of PF_6^- at 841 and 559 cm^{-1}.[6] In the IR spectra of **3**, **6**, and **7**, the ν(C≡N) band of K[Au(CN)$_2$][22] at 2141 cm^{-1} was split into one weak band at 2156 cm^{-1} (**3**, **6**, and **7**) and one strong band at 2137 cm^{-1} (**3** and **5**) and 2133 cm^{-1} (**6**) because the $[Au(CN)_2]^-$ anion was dimerized into the $[Au(CN)_2]_2^{2-}$ dianion in **3**, **6**, and **7**. The ^{1}H NMR spectra of **1**−**3**, **6**, and **7** in DMSO-d_6 at room temperature showed a multiplet for protons of Ph groups at 7.59−7.74 ppm and a singlet related to protons of NMe_3 at ca. 3.51 ppm.

The electronic spectra of **1**−**3**, **6**, and **7** in DMF exhibited strong and broad absorptions at 304 nm (**1**), 302 nm (**2**), 302 nm (**3**), 296 nm (**6**), and 268 nm (**7**) (see the Supporting Information). Because the absorption spectral data for K[Au(CN)$_2$] showed no absorption above 250 cm^{-1} with low concentration (10^{-4} M)[23] and the absorption spectrum of the free Tab in DMF had a broad absorption band at 320 nm,[6b] the peaks observed in the spectra of **1**−**3**, **6**, and **7** are all blue-shifted and may be due to the ligand (Tab)-to-metal charge transfer (LMCT).

Preliminary photochemical and photophysical investigation of **1**−**3**, **6**, and **7** revealed very interesting photoluminescent properties in the solid state at ambient temperature (Figure 8). The emission spectrum (λ_{ex}^{max} = 375 nm) of **1** displayed one small band at 450 nm and another emission band at 534 nm, while (λ_{ex}^{max} = 360 nm) of **2** displayed one small band at 450 nm and another broad emission band at 650 nm. Excitation of **3** at 399 nm resulted in one emission band at 450 nm and another more broad and intense emission band at 674 nm with two small shoulders at 507 and 540 nm. **6** and **7** exhibited emission bands at 528 (**6**) and 522 (**7**) nm with excitation at 380 (**6**) and 466 (**7**) nm. The lifetimes were measured by time-resolved spectroscopy at room temperature and calculated through the monoexponential decay method. Being emitted at 450 nm, the lifetimes of **1**−**3** were measured to be 0.42 μs (**1**), 3.10 μs (**2**), and 1.33 μs (**3**), while those of **6** and **7** were 0.24 and 0.10 μs, respectively. The higher-energy emission band at 450 nm in **1**−**3** may be due to the metal-centered (MC) excited state,[1k] while the lower-energy one at 534 nm in **1**, 650 nm in **2**, or 674 nm in **3** may be due to the ligand-to-metal−metal charge transfer.[24] The different emission bands between **1** and **2** may be due to the different anions as well as the H_2O molecules.[25] Solid K[Au(CN)$_2$] had one emission band at 390 nm.[1a,2a] As discussed previously, **4** showed weak emission bands at 442 and 533 nm[6a] while **5** had no luminescence. Thus, the emission bands of **6** and **7** are likely to be the MC excited state (originated from the $[Au(CN)_2]_2^{2-}$ part), though the weak S → Ag LMCT may not be ruled out in **6**. In this context, the two small shoulders in **3** may also be ascribed to the MC excited states derived from the $[Au(CN)_2]_2^{2-}$ part. It is noted that the solutions of **1**−**3**, **6**, and **7** did not show luminescence, which may be due to the fact that these compounds, when dissolved, tend to dissociate into nonemissive monomeric species, in which the ionic interactions and aurophilic bonding interactions may no longer be present.[26]

Conclusions

In this paper, we have demonstrated a route to rational construction of two tetranuclear metal string compounds **3** and **6** from reactions of preformed complexes **2** and **4** with K[Au(CN)$_2$]. Compound **3** or **6** has a ligand-unassisted Au_4 or Ag_2Au_2 string structure in which two {[(Tab)$_2$M][Au(CN)$_2$]} species (formed through ionic interaction between the $[M(Tab)_2]^+$ cation and the $[Au(CN)_2]^-$ anion) are held together by one Au−Au aurophilic bonding interaction. **3** and **6** represent the interesting examples in which ionic interactions and aurophilic interactions are designed to work perfectly on a same string structure in a cooperative way. It is noteworthy that the orientation of the $^-SC_6H_4NMe_3^+$ groups coordinated at Au atoms of **2** is retained in the structure of **3** while those of **4** are reoriented in the same direction during the reaction so as to facilitate the formation of the string structure of **6**. Although the reaction of **5** with K[Au(CN)$_2$] did not result in the formation of our expected

(22) Chadwick, B. M.; Frankiss, S. G. *J. Mol. Struct.* **1976**, *31*, 1−7.
(23) Rawashdeh-Omary, M. A.; Omary, M. A.; Patterson, H. H. *J. Am. Chem. Soc.* **2000**, *122*, 10371−10380.
(24) (a) Pan, Q. J.; Zhang, H. X. *Organometallics* **2004**, *23*, 5198−5209. (b) Bardaji, M.; Calhorda, M. J.; Costa, P. J.; Jones, P. G.; Laguna, A.; Perez, M. R.; Villacampa, M. D. *Inorg. Chem.* **2006**, *45*, 1059−1068.
(25) (a) Charbonnière, L. J.; Ziessel, R.; Montalti, M.; Prodi, L.; Zaccheroni, N.; Boehme, C.; Wipff, G. *J. Am. Chem. Soc.* **2002**, *124*, 7779−7788. (b) Coker, N. L.; Krause Bauer, J. A.; Elder, R. C. *J. Am. Chem. Soc.* **2004**, *126*, 12−13. (c) Anzenbacher, P., Jr.; Tyson, D. S.; Jursikova, K.; Castellano, F. N. *J. Am. Chem. Soc.* **2002**, *124*, 6232−6233. (d) Supkowski, R. M.; Horrocks, W. D., Jr. *Inorg. Chem.* **1999**, *38*, 5616−5619. (e) Klonkowski, A. M.; Lis, S.; Pietraszkiewicz, M.; Hnatejko, Z.; Czarnobaj, K.; Elbanowski, M. *Chem. Mater.* **2003**, *15*, 656−663.
(26) King, C.; Wang, J. C.; Khan, M. N. I.; Fackler, J. P., Jr. *Inorg. Chem.* **1989**, *28*, 2145−2149.

Au_2Hg_2 string complex, the unexpected complex **7** has an interesting 1D chain structure where the $[Hg(Tab)_2]^{2+}$ dication and the $[Au(CN)_2]_2^{2-}$ dianion are interconnected by the secondary Hg···N(CN) interactions. Relative to those of their corresponding precursors, **3**, **6**, and **7** showed more intensive luminescence in the solid state. The incorporation of a preformed luminescent precursor such as **2** and $[Au(CN)_2]^-$ into the desired structures may be an effective method for the preparation of other luminescent materials. Works toward this respect are underway.

Acknowledgment. This work was supported by the NNSF of China (Grants 20271036 and 20525101), the NSF of Jiangsu Province (Grant BK2004205), the Specialized Research Fund for the Doctoral Program of Higher Education (Grant 20050285004), the Qin-Lan Project of Jiangsu Province, and the State Key Laboratory of Coordination Chemistry, Nanjing University, in China. The authors also highly appreciated some useful suggestions from the Editor and the reviewers.

Supporting Information Available: Crystallographic data of compounds **1**−**3**, **6**, and **7** (CIF), hydrogen-bond geometry in **1**−**3**, **6**, and **7**, the 2D structure formed via hydrogen-bonding interactions in **1**, the 3D structure formed via C−H···F hydrogen-bonding interactions in **2**, the arrangement of the Au_4 strings in the crystal of **3**, the 1D structure formed via C−H···Au hydrogen-bonding interactions in **3**, the view of the molecular structure of **6**, the 1D structure formed via C−H···Ag hydrogen-bonding interactions in **6**, the 3D structure formed via all hydrogen-bonding interactions in **6**, the 2D network formed via Hg···N secondary interactions and hydrogen-bonding interactions in **7**, the thermogravimetric analysis curves for **1**−**3**, **6**, **7**, and Tab, and the absorption spectra of **1**−**3**, **6**, and **7** (in PDF format). This material is available free of charge via the Internet at http://pubs.acs.org.

IC060655M